Dynamics of Water Associated with Lithium Ions Distributed in Polyethylene Oxide

Zhe Zhang, Michael Ohl, Souleymane O. Diallo, Niina H. Jalarvo, Kunlun Hong, Youngkyu Han, Gregory S. Smith, and Changwoo Do

Phys. Rev. Lett. **115**, 198301 — Published 3 November 2015

DOI: 10.1103/PhysRevLett.115.198301

Dynamics of Water Associated with Lithium Ions Distributed in Poly (Ethylene Oxide)

Zhe Zhang[1,2], Michael Ohl[2], Souleymane O. Diallo[3], Niina H. Jalarvo[2,4], Kunlun-Hong[5], Youngkyu Han[1], Gregory S. Smith[1], Changwoo Do[1,*]

[1]Biology and Soft-Matter Division, Oak Ridge National Laboratory, Oak Ridge, TN 37831, USA

[2]Forschungszentrum Jülich, Jülich Center for Neutron Science, Outstation at the Spallation Neutron Source (SNS), Oak Ridge National Laboratory, Oak Ridge TN 37831, USA

[3]Quantum Condensed Matter Division, Oak Ridge National Laboratory, Oak Ridge, TN 37831, USA

[4]Chemical and Engineering Materials Division, Neutron Sciences Directorate, Oak Ridge National Laboratory, Oak Ridge, TN 37831, USA

[5]Center For Nanophase Materials Sciences Division, Oak Ridge National Laboratory, Oak Ridge, TN 37831, USA

The dynamics of water in the Poly (ethylene oxide) (PEO)/LiCl solution has been studied with quasi-elastic neutron scattering (QENS) experiments and molecular dynamics (MD) simulations. Two different time scales of water diffusion representing interfacial water and bulk water dynamics have been identified. The measured diffusion coefficient of interfacial water remained 5~10 times smaller than that of bulk water but both were slowed by approximately 50% in the presence of Li^+. Detailed analysis of MD trajectories suggest that Li^+ are favorably found at the surface of hydration layer, and the probability to find the caged Li^+ configuration formed by the PEO is lower than for the non-caged Li^+-PEO configuration. In both configurations, however, the slowing down of water molecules is driven by reorienting water molecules and creating water-Li^+ hydration complexes. Performing the MD simulation with different ions (Na^+ and K^+) revealed that smaller ionic radius of the ions is a key factor in disrupting the formation of PEO cages by allowing spaces for water molecules to come in between the ion and PEO.

Water and water-containing systems are ubiquitous in nature. Water plays an essential role in many physical processes [1,2], and chemical reactions [3,4] as well as biological properties [5-9]. Generally, water can be categorized into two populations in water-containing systems: bulk water and interfacial water [10,11]. The bulk water molecules exist away from the solute or the interfaces where atomistic and molecular interactions with them can be ignored [11,12], while the interfacial water molecules are usually found near the solute or interfaces having properties different from bulk water [13-19]. The interfacial water molecules often demonstrate extraordinary structural and dynamical properties compared to those of the bulk water molecules[14,18,19], and efforts are still being made to understand the structure and dynamics of interfacial water under various confinement [20].

The role of water in polymeric systems with salts has long been investigated in soft matter research for both fundamental science and application development. The properties of polymers and ions in these systems have shown strong dependencies on the structure and dynamics of interfacial water (or hydration water) molecules. For example, the forward rate of proton hopping in Nafion is known to be determined by the orientational dynamics of water near the polymer [21]. In solid polymer electrolyte batteries [22-24] based on poly (ethylene oxide) (PEO) and lithium, it has been reported that hydrating PEO increases the conductivity by as much as 1000 times that of the typical binary mixture of PEO/lithium salts [25,26]. Such enhancement was attributed to water absorption, which increases the mobility of PEO chains producing more free mobile ions by reducing the coordination between PEO and cations [26,27]. Therefore understanding the insight of water dynamics associated with Li^+ distribution in aqueous PEO/Li^+ solution can provide a big potential of developing lithium-batteries with high conductivity and capacity. Further more, studying the interplay among water, salts and polymer will result in an important guidance for the desired functional materials.

Although water dynamics is playing a critical role on the function of the materials, which can be seen directly from the above examples, however, most of the focus has been given to the influence of water on the behaviors of polymers and ions, but much less attention has been made to the structure and dynamics of water itself, i.e. what is the effect on water dynamics from polymers and ions? In order to answer this question, a detailed analysis of water dynamics associated with microstructure of polymer-ions-water complex is needed. Among polymers, PEO has important applications to medical use [28-31] in human or animal bodies which include abundance of water and ions, as well as to energy storage applications. Therefore, PEO-ion-water complex has been chosen as a model system to study water dynamics influenced by surrounding polymers and ions.

Neutron scattering and molecular dynamics (MD) simulation have been widely used to study water dynamics in the past years [32-34]. The energy of neutrons and large incoherent scattering cross section of hydrogen made quasi-elastic neutron scattering a powerful tool for accessing dynamics of water in sub ps to ns time scales. By having similar length and time scales, atomistic MD simulation is a complimentary tool to neutron scattering to obtain experimentally inaccessible information such as atom positions and dynamics [24,35,36]. Here, we use quasi-

elastic neutron scattering (QENS) and MD simulations to study a PEO/water mixture (wt% = 50%) with and without lithium salts (LiCl) (Molar ratio EO:Li^+ = 10:1).

In this study, water can be clearly categorized into bulk water and interfacial water by the boundary of hydration layer at R = 4 Å, where R is the distance between water molecule and PEO chains (Supplemental Material [37], which includes references [12,38-57]). Recent studies by broadband dielectric spectroscopy, nuclear magnetic resonance (NMR) and MD simulation have shown bulk water and interfacial water have significant heterogeneity [58-62], especially alpha and beta relaxation process. Beta-relaxation process is a local process which can be observed below the glass transition temperature (T_g<175K [58]), and usually merges with alpha-relaxation process above T_g [58,63]. The QENS experiment was taken at T=300K in this study, which is much higher than T_g, thus only alpha-relaxation is visible in the experiment. Therefore two dynamic scales, representing bulk and interfacial water, in both QENS and MD simulation have been considered by two Lorentzian functions when modeling the dynamic structure factor, $S(q, E)$ where E is the energy in Fourier transform [37] and q is wave vector. Following the approaches by Barnes and Leyte [46], the dynamic structure factor at each q is given as

——— ——— (1)

where Γ_1 and Γ_2 are the widths of the Lorentzian curves representing the dynamics for bulk and interfacial water, respectively. f is the fraction of interfacial water. In general, the dynamics of bulk water molecules are described by combinations of rotational diffusion and translation diffusion processes [54,64]. However, within the q range and energy range explored by BASiS (0.3 $Å^{-1} < q < 1.1$ $Å^{-1}$, -115 μeV < E < 115 μeV), the rotational diffusion can be neglected and therefore, the bulk water diffusion process can be approximated by pure translational diffusion, which can be given by $\Gamma_1 = D_1 q^2$, where D_1 is the q-independent diffusion coefficient. Thus $S(q, E)$ with different q values were simultaneously fit with a single D_1. Examples (q = 0.5 $Å^{-1}$) of successful data fitting results are shown in Fig. 1(a) (from QENS experiments) and Fig. 1(b) (from MD simulation), respectively (the detailed fitting procedures and fitting results can be found in Supplemental Material [37]). Fitting with two Lorentzian functions (Eq. (1)) resulted in excellent agreement with both of the QENS data and the MD simulation data as shown in these figures supporting existence of two dynamic processes. The range of energy axis of MD simulation in Fig. 1(b) is different from that of QENS experiment, because the MD simulation explored larger energy spectrum where the broadening due to the rotational motion of water molecules can also be seen (Fig. 1(b), green and purple lines). The rotational motion of water molecules was modeled with an infinite stretched exponential series when calculating the intermediate scattering function, and in order to reduce the calculation time, only the first two terms of the series were considered in the fitting procedure [37,53,54]. The fitted Γ_2 using Eq. (1) are shown in Fig. 1(c) and 1(d) for selected q values. Dramatic slowing down of the dynamic process by half is clearly observed when LiCl was added to the system from both the experiments and simulations. Γ_2 is also found to follow $\Gamma_2 = D_2 q^2$ in both PEO/water and PEO/water/LiCl systems, suggesting that the diffusion process can be characterized by the q-independent translational diffusion coefficient D_2. This indicates that the presence of LiCl only influences the dynamics scales but does not change the fundamental characters of the motion. The diffusion coefficients estimated from the fitting are summarized in Supplemental Material [37].

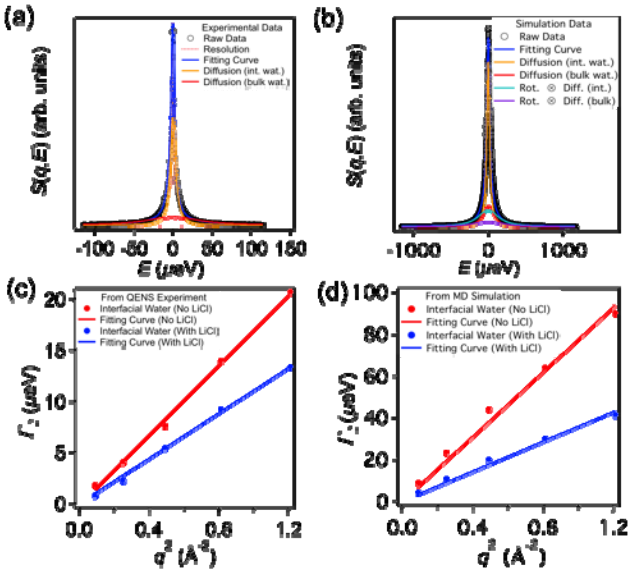

FIG. 1 (color online). Comparison of QENS Experiment and MD Simulation. (a) Data fitting of QENS Experiment (PEO/water solution without LiCl at q = 0.5 $Å^{-1}$); (b) Data fitting of MD simulation (PEO/water solution without LiCl at q = 0.5 $Å^{-1}$)*; (c) Linear fitting of Γ_2 vs. q^2 (interfacial water) obtained from QENS experiment; (d) Linear fitting of Γ_2 vs. q^2 (interfacial water) obtained from MD simulation.

*compared to the other two components, the rotational component is very flat, in order to give a better representation, the amplitude of the peak was zoomed in by ×10.

The diffusion coefficient of the bulk water obtained from the QENS and MD simulation agree with known values from literatures. However, the values from MD simulation is about twice larger than the experimental value [65-68], where such quantitative discrepancy is generally understood by the fact that the MD simulation is using an effective interaction potential to describe the dynamic properties of the system, which is a simplified model; while

the QENS experiments measure the details of the molecular interaction directly in the solution [69]. Borodin and collaborators [64] reported the concentration dependence of water dynamics in PEO/water solution by MD simulation. The diffusion coefficient of interfacial water which was estimated to be 1×10^{-5} cm^2/s at 50 wt% PEO, is consistent with the number we obtained from our MD simulation analysis. From MD simulation, the fraction of interfacial water molecules can be estimated by counting the number of water molecules within the hydration layer defined by the distance 4 Å [37]. On average, 68% of water molecules are found to be interfacial water based on our MD trajectory analysis. This fraction is very close to the fraction of interfacial water (f = 73%) obtained from QENS experiment, again suggesting that MD simulation and QENS experiment are in good agreement.

In bulk, the reorientation of water molecules toward to Li^+ and the formation of hydration complexes (Li^+-water) [37] are responsible for the dynamic slow-down of water molecules as well as the increased viscosity, which has been noted by Stirnemann and coworkers in their study on water/ion solution [57]. The Li^+ however, does not remain in bulk or near interfaces of polymers but changes its position over time influencing the dynamics of both the bulk and the interfacial water molecules. For example, distances from PEO to the selected Li^+ ions have been traced and representative data are shown in Fig. 2(a). It is interesting to note that whenever Li^+ are at the closest distance from PEO (~ 2 Å), they stay longer than when they are away from PEO. For example, Li 617 (orange) remains at a distance of 2 Å for almost 1 ns at the beginning, then goes to the bulk region. Based on the fluctuations of the distance from 1 ns to 3.5 ns, it is also clear that Li 617 moves in and out of the hydration layer (R ~ 4 Å) quite frequently. When its distance becomes ~ 2 Å again at around 4 ns, a brief moment of constant distance is again observed. Similar observations are commonly found in other Li^+ in the same plot. Li 616 exhibits longer residing time at the closest distance and fluctuates between hydration layer and bulk region. Li 630 mostly stays under the hydration layer, while Li 618 shows more dramatic motions moving in and out of the hydration boundaries. Three distinctive types of motion can be identified from this observation. First, when Li^+ are at closest distance from PEO, they are trapped longer than usual. Second, Li^+ tends to spend significant amount of time at a distance of 4 Å, which is the hydration layer boundary. Third, Li^+ move in and out of the hydration boundary therefore interacting with both the interfacial water molecules and the bulk water molecules. These characteristics are also found in statistically averaged quantities like pair distribution function of Li^+ with the respect of PEO, $g(r)_{Li\text{-}PEO}$ (Fig. 2(b)). The peak at 2 Å corresponds to the trapped Li^+, and the broader peak at 4 Å represents Li^+ that are more frequently found near the hydration layer boundaries. The distribution of total time that Li^+ spend at various distances from PEO (*t-R* distribution) is also calculated and shows that Li^+ spend most of their time near the hydration layer boundary which is around 4 Å. The preferential appearance at short distance (2 Å) is observed clearly as well, suggesting caging by PEO as in the pair distribution function. (Fig. 2(c))

The representative spatial configurations for trapped Li^+ and the Li^+ at the hydration layer boundaries are captured in the snapshots shown in Fig. 2(d)-(f). The trapped Li^+ in fact shows the Li^+ caged by the PEO due to the strong interaction between Li^+ and the oxygen atoms of PEO [24,70,71]. The segmental motion of PEO, which is determined by the solvent viscosity and temperature, promotes a longer residing time for the caged configuration [24]. Although Li^+ is caged (Fig. 2(d)), it still influences nearby water molecules such as water 812 (first nearest neighbor), water 1155, and water 669 (second nearest neighbor) contributing to the overall dynamics of water. When Li^+ is at the hydration layer boundary (Fig. 2(e)-(f)), interaction of Li^+ with both of the interfacial water molecules (water 697, water 1123, and water 1186) and the bulk water molecules (water 932 and water 1144) is observed. The interfacial water molecules which are strongly bounded by the PEO contribute to form Li^+-water complexes resulting in Li^+ distribution bounded to the hydration layer. This microstructure of the Li^+-water complex is practically the same as that in bulk, which indicates that the dynamic slowing-down process for interfacial water in principle is very similar to that in bulk region.

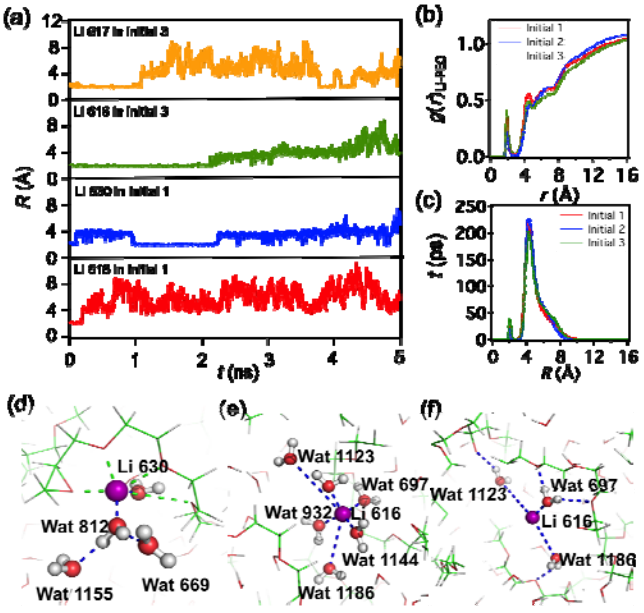

FIG. 2 (color online). Li^+ distribution with the respect of distance to PEO. (a) Distances of four Li^+ from PEO during simulation. R = 4 Å is the boundary of the hydration layer. Three different initial structures (Initial 1, Initial 2, and Initial 3) have been used for the MD simulation to ensure validity of the simulation results. (b) Pair distribution function of Li^+ with the respect of PEO; (c) The distribution of total time that Li^+ spends at various distances from PEO. In (d)-(f): green-red lines represented PEO (green: carbon atoms; red: oxygen atoms); purple ball represented Li^+; dash lines indicated the interaction between two atoms (green: interaction between Li^+ and PEO; blue: interactions involved in water, i.e. water and PEO, water and Li^+, or water and water). (d) A snap shot (t = 1500 ps) of PEO-Li^+_{630}-water complex when the Li^+ was trapped by PEO; (e)-(f) A snap shot (t = 3825 ps) of PEO-Li^+_{616}-water complex when the Li^+ (Li 616) was located at the boundary of the hydration layer. (e) and (f) represent the same complex viewed from different angles, in particular (f) is aimed to indicate Wat 697, Wat 1123, and Wat 1186 within the hydration layer.

Generally speaking, monovalent cations could have distinct behavior due to their size [72,73]. In order to better understand what influences the relative probability of Li^+ being in the caged configuration or the hydration layer boundaries, additional simulations with different ions of the same charge have been performed. After the same series of simulations with Na^+ and K^+ replacing Li^+, the *t-R* distributions were calculated (Fig. 3(a) and 3(b)). It is very clear that in aqueous PEO/NaCl and PEO/KCl solutions, the ion-caging effect is much stronger and dominant than in PEO/LiCl solution. While the *t-R* distribution does not differentiate stationary ions and moving ions explicitly, the relative comparison of the amplitude of this distribution still enables comparison of relative trapping time of ions. The *t-R* distribution suggests that on average Na^+ ion was trapped for ~ 380 ps total, while K^+ ions spent longer time (> 400 ps total) at distance R = 2 Å. (Fig 3(a) and 3(b)) By inspecting individual ions trajectory, it was also confirmed that K^+ ions stay indeed longer in the cages (R = 2 Å). (insets of Fig 3(a) and 3(b)) While these ions were also observed near the hydration layer boundaries as indicated by the peaks around 4 Å, a caged configuration is found to be much more dominant compared to the Li^+ case. The number of ions which has ever been captured (based on the distance, $R \leq 3$ Å) by more than 3 EO monomers during 5 ns simulation can be directly counted. It turns out that more than half (13) of K+ ions out of 24 have been caged, while the number of caged ions become less for smaller ions, i.e. 9 and 2 for Na+ and Li+, respectively [37]. The total time that these ions spend while being caged is also found to be longest for the K^+ ions (4.4 ns) and shortest for the Li^+ (0.64ns) [37]. These estimations indicate that the ions with large ionic radius not only form the cages easily but also stay within the cages longer than the smaller ions. By examining the caging structure for Na^+ and K^+ represented by the ionic radii as shown in Fig. 3c and 3d, we found that less volume is available for water molecules to come in between the ions and the surrounding polymers. Water is competing with PEO for ions, thus is playing an important role to break PEO cages, which can be seen from the fact that the number of water molecules surrounding caged ions is less than that of noncaged ions [37]. We believe that as the size of ions become larger, it become more difficult for the water molecules to penetrate between ions and PEO, reducing the chances of disrupting the ion-PEO interactions and slowing down the segmental motions of PEO. Thus, it becomes difficult to release ions from the cages and slows down ion transportation. These observations agree with the well-known fact that Li^+ among many other ions produces the best ionic conductivities in PEO-based solid polymer electrolyte batteries [25]. In addition, our simulation also confirms that the cage-opening and closing plays an essential role in assisting ion transportations in polymer electrolytes [24].

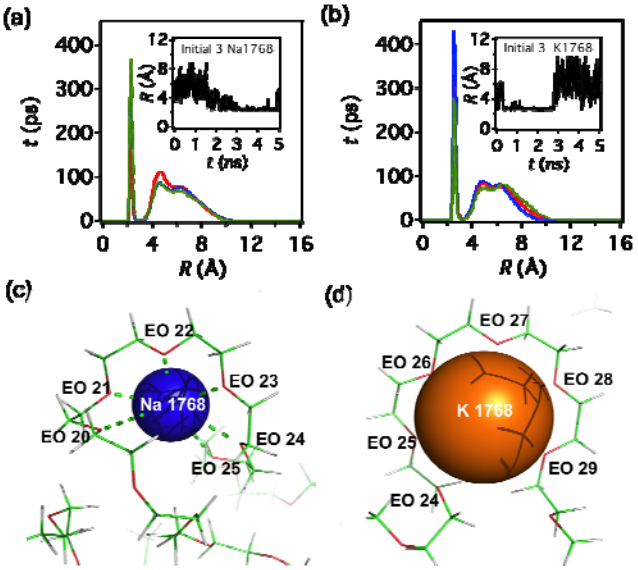

FIG. 3 (color online). Trapping Na^+ and K^+. (a) Temporal distribution of Na^+ along with their distance from PEO chains: Red: Initial 1; Blue: Initial 2; and Green: Initial 3. The inset represented an example (Na 1768 from Initial 3); (b) Temporal distribution of K^+ along with their distance from PEO chains: Red: Initial 1; Blue: Initial 2; and Green: Initial 3. The inset represented an example (K 1768 from Initial 3); (c) A snap shot of Na 1768 (blue ball) from Initial 3 at t = 4000ps; PEO was represented with green-red lines and the dash line represented the interaction between Na 1768 and residues in PEO ("EO" represented PEO residue: ethylene oxide; and the number was the residue ID). (d) A snap-shot of K 1768 (orange ball) from Initial 3 at t = 1500 ps. PEO was represented with green-red lines. The interaction dash line was not shown due to small space inside of the cage.

In aqueous PEO/LiCl solution, we observe that the water dynamics both in bulk and at the interfaces of PEO were dramatically slowed down by almost half with both

QENS experiment and MD simulation. Detailed investigation of the MD trajectories reveals that Li^+ are more frequently found in the hydration layer boundaries interacting with both of the interfacial water molecules and the bulk water molecules. By replacing Li^+ with Na^+ or K^+, the caged ion-PEO complex became a major microstructure due to the bigger ionic radius which prevents water molecules from coming in for disruption of the cage conformation. To our knowledge, this is the first study providing detailed process of dynamics changes of water molecules influenced by ions both in bulk and near the interfaces. The revealed interplay of water molecules and ion-PEO complex structures will provide valuable insights in designing polymer-based ion batteries.

The Research at Oak Ridge National Laboratory's Spallation Neutron Source was sponsored by the Scientific User Facilities Division, Office of Basic Energy Sciences, U.S. Department of Energy. The author, Zhe Zhang, gratefully acknowledges the financial support from Jülich Center for Neutron Science, Research center Jülich. The authors gratefully thank Dr. E. Mamontov and Dr. W.-R. Chen for their input and valuable discussions.

[1] J. C. Palmer, F. Martelli, Y. Liu, R. Car, A. Z. Panagiotopoulos, and P. G. Debenedetti, Nature **510**, 385 (2014).
[2] E. B. Moore and V. Molinero, Nature **479**, 506 (2011).
[3] M. Maroncelli, J. Macinnis, and G. R. Fleming, Science **243**, 1674 (1989).
[4] I. Ohmine and S. Saito, Acc. Chem. Res. **32**, 741 (1999).
[5] R. H. Zhou, X. H. Huang, C. J. Margulis, and B. J. Berne, Science **305**, 1605 (2004).
[6] F. T. Burling, W. I. Weis, K. M. Flaherty, and A. T. Brunger, Science **271**, 72 (1996).
[7] J. P. Lin, I. A. Balabin, and D. N. Beratan, Science **310**, 1311 (2005).
[8] J. Tian and A. E. Garcia, J. Am. Chem. Soc. **133**, 15157 (2011).
[9] J. A. Lemkul and D. R. Bevan, J. Phys. Chem. B **114**, 1652 (2010).
[10] M. F. Kropman and H. J. Bakker, Science **291**, 2118 (2001).
[11] J. Israelachvili and H. Wennerstrom, Nature **379**, 219 (1996).
[12] B. Bagchi, Chem. Rev. **105**, 3197 (2005).
[13] J. Song, J. Franck, P. Pincus, M. W. Kim, and S. Han, J. Am. Chem. Soc. **136**, 2642 (2014).
[14] T. Shikata, M. Okuzono, and N. Sugimoto, Macromolecules **46**, 1956 (2013).
[15] J. H. Tian and A. E. Garcia, Biophys. J. **96**, L57 (2009).
[16] J. H. Tian and A. E. Garcia, J. Chem. Phys. **134** (2011).
[17] G. Hummer, J. C. Rasaiah, and J. P. Noworyta, Nature **414**, 188 (2001).
[18] J. K. Holt, H. G. Park, Y. Wang, M. Stadermann, A. B. Artyukhin, C. P. Grigoropoulos, A. Noy, and O. Bakajin, Science **312**, 1034 (2006).
[19] D. Z. Liu, Y. Zhang, C. C. Chen, C. Y. Mou, P. H. Poole, and S. H. Chen, Proc. Natl. Acad. Sci. U.S.A. **104**, 9570 (2007).
[20] A. Paciaroni, M. Casciola, E. Cornicchi, M. Marconi, G. Onori, M. Pica, R. Narducci, A. De Francesco, and A. Orecchini, J. Phys-Condens. Mat. **18**, S2029 (2006).
[21] M. K. Petersen, A. J. Hatt, and G. A. Voth, J. Phys. Chem. B **112**, 7754 (2008).
[22] O. Borodin and G. D. Smith, Macromolecules **33**, 2273 (2000).
[23] J. K. Hyun, H. T. Dong, C. P. Rhodes, R. Frech, and R. A. Wheeler, J. Phys. Chem. B **105**, 3329 (2001).
[24] C. Do, P. Lunkenheimer, D. Diddens, M. Gotz, M. Weiss, A. Loidl, X. G. Sun, J. Allgaier, and M. Ohl, Phys. Rev. Lett. **111**, 018301 (2013).
[25] F. L. Tanzella, W. Bailey, D. Frydrych, G. C. Farrington, and H. S. Story, Sol. Stat. Ion. **5**, 681 (1981).
[26] S. A. Hashmi, J. Mater. Sci. **33**, 989 (1998).
[27] Z. Tao and P. T. Cummings, Mol. Simulat. **33**, 1255 (2007).
[28] R. Langer and D. A. Tirrell, Nature **428**, 487 (2004).
[29] R. Langer, Nature **392**, 5 (1998).
[30] R. Langer, Science **293**, 58 (2001).
[31] T. L. Krause and G. D. Bittner, Proc. Natl. Acad. Sci. U.S.A. **87**, 1471 (1990).
[32] S. H. Chen, L. Liu, E. Fratini, P. Baglioni, A. Faraone, and E. Mamontov, Proc. Natl. Acad. Sci. U.S.A. **103**, 9012 (2006).
[33] R. Bergman and J. Swenson, Nature **403**, 283 (2000).
[34] A. Kalra, S. Garde, and G. Hummer, Proc. Natl. Acad. Sci. U.S.A. **100**, 10175 (2003).
[35] L. Hong, D. C. Glass, J. D. Nickels, S. Perticaroli, Z. Yi, T. Madhusudan, H. O'Neill, Q. Zhang, A. P. Sokolov, and J. C. Smith, Phys. Rev. Lett. **110**, 028104 (2013).
[36] L. Hong, N. Smolin, and J. C. Smith, Phys. Rev. Lett. **112**, 158102 (2014).
[37] See Supplemental Material at http://link.aps.org/supplemental/XX.XXXX/PhysRevLett.XXX.XXXXXX, which includes Refs [12, 38-57].
[38] E. Mamontov and K. W. Herwig, Rev. Sci. Instrum. **82** (2011).
[39] H. Bekker, H. J. C. Berendsen, E. J. Dijkstra, S. Achterop, R. Vondrumen, D. Vanderspoel, A. Sijbers, H. Keegstra, B. Reitsma, and M. K. R. Renardus, Phys. Comp. '92, 252 (1993).
[40] D. Van Der Spoel, E. Lindahl, B. Hess, G. Groenhof, A. E. Mark, and H. J. Berendsen, J. Comput. Chem. **26**, 1701 (2005).
[41] B. Hess, C. Kutzner, D. van der Spoel, and E. Lindahl, J. Chem. Theory Comput. **4**, 435 (2008).
[42] W. L. Jorgensen and J. Tiradorives, J. Am. Chem. Soc. **110**, 1657 (1988).
[43] W. L. Jorgensen, D. S. Maxwell, and J. TiradoRives, J. Am. Chem. Soc. **118**, 11225 (1996).
[44] G. Bussi, D. Donadio, and M. Parrinello, J. Chem. Phys. **126** (2007).
[45] S. Melchionna, Phys. Rev. E **61**, 6165 (2000).
[46] A. C. Barnes, T. W. N. Bieze, J. E. Enderby, and J. C. Leyte, J. Phys. Chem-Us **98**, 11527 (1994).
[47] B. Wu, Y. Liu, X. Li, E. Mamontov, A. I. Kolesnikov, S. O. Diallo, C. Do, L. Porcar, K. L. Hong, S. C. Smith *et al.*, J. Am. Chem. Soc. **135**, 5111 (2013).
[48] B. Wu, B. Kerkeni, T. Egami, C. Do, Y. Liu, Y. M. Wang, L. Porcar, K. L. Hong, S. C. Smith, E. L. Liu *et al.*, J. Chem. Phys. **136**, 144901 (2012).

[49] S. Dixit, J. Crain, W. C. Poon, J. L. Finney, and A. K. Soper, Nature **416**, 829 (2002).
[50] Y. Ding, A. A. Hassanali, and M. Parrinello, Proc. Natl. Acad. Sci. U.S.A. **111**, 3310 (2014).
[51] T. Rog, K. Murzyn, K. Hinsen, and G. R. Kneller, J. Comput. Chem. **24**, 657 (2003).
[52] B. J. Drouin, S. S. Yu, J. C. Pearson, and H. Gupta, J. Mol. Struct. **1006**, 2 (2011).
[53] E. Mamontov, Chem. Phys. Lett. **530**, 55 (2012).
[54] S. Mitra, R. Mukhopadhyay, I. Tsukushi, and S. Ikeda, J. Phys-Condens. Mat. **13**, 8455 (2001).
[55] O. Borodin, F. Trouw, D. Bedrov, and G. D. Smith, J. Phys. Chem. B **106**, 5184 (2002).
[56] S. B. Rempe, L. R. Pratt, G. Hummer, J. D. Kress, R. L. Martin, and A. Redondo, J. Am. Chem. Soc. **122**, 966 (2000).
[57] G. Stirnemann, E. Wernersson, P. Jungwirth, and D. Laage, J. Am. Chem. Soc. **135**, 11824 (2013).
[58] S. Cerveny, G. A. Schwartz, R. Bergman, and J. Swenson, Phys. Rev. Lett. **93**, 245702 (2004).
[59] S. Cerveny, A. Alegria, and J. Colmenero, Phys. Rev. E 77, 031803 (2008).
[60] J. Swenson and S. Cerveny, J. Phys-Condens. Mat. **27** (2015).
[61] M. Rosenstihl, K. Kampf, F. Klameth, M. Sattig, and M. Vogel, J. Non-Cryst. Solids **407**, 449 (2015).
[62] S. Khodadadi, S. Pawlus, and A. P. Sokolov, J. Phys. Chem. B **112**, 14273 (2008).
[63] G. D. Smith and D. Bedrov, J. Polym. Sci., Part B: Polym. Phys. **45**, 627 (2007).
[64] O. Borodin, D. Bedrov, and G. D. Smith, J. Phys. Chem. B **106**, 5194 (2002).
[65] Q. Liu, R. K. Schmidt, B. Teo, P. A. Karplus, and J. W. Brady, J. Am. Chem. Soc. **119**, 7851 (1997).
[66] W. L. Jorgensen and C. Jenson, J. Comput. Chem. **19**, 1179 (1998).
[67] P. E. Smith, H. D. Blatt, and B. M. Pettitt, J. Phys. Chem. B **101**, 3886 (1997).
[68] M. Holz, S. R. Heil, and A. Sacco, Phys. Chem. Chem. Phys. **2**, 4740 (2000).
[69] E. Guarini, M. Sampoli, G. Venturi, U. Bafile, and F. Barocchi, Phys. Rev. Lett. **99**, 167801 (2007).
[70] P. R. Chinnam and S. L. Wunder, J. Mater. Chem. A **1**, 1731 (2013).
[71] J. M. Tarascon and M. Armand, Nature **414**, 359 (2001).
[72] S. E. Kim, I. B. Lee, C. Hyeon, and S. C. Hong, J. Phys. Chem. B **118**, 4753 (2014).
[73] A. V. Egorov, A. V. Komolkin, V. I. Chizhik, P. V. Yushmanov, A. P. Lyubartsev, and A. Laaksonen, J. Phys. Chem. B **107**, 3234 (2003).